

1 **INDO-BURMESE COLLISION OCCURRED AT EOCENE EVIDENCE FROM THE**  
2 **DETRITAL FISSION TRACK THERMOCHRONOLOGY OF NORTHEAST INDIA**

3  
4 Ramamoorthy Ayyamperumal<sup>1,2\*</sup>, Ramasamy Sooriamuthu<sup>2</sup>,  
5 Gnanachandrasamy Gopalakrishnan<sup>3</sup>, Nusrat Nazir<sup>4</sup>, Xiaozhong Huang<sup>1</sup>  
6

7 <sup>1</sup>Key Laboratory of Western China's Environmental system, College of Earth and  
8 Environmental Sciences, Lanzhou University, Lanzhou-730000, P.R.China.

9 <sup>2</sup>Department of Geology, School of earth and atmospheric sciences, University of Madras,  
10 Guindy campus, Chennai-India 600025

11 <sup>3</sup>School of Geography and Planning, Sun Yat-Sen University, Guangzhou, 510275, P.R.  
12 China.

13 <sup>4</sup>School of Earth Sciences, Lanzhou University, Lanzhou-730000, P.R. China.  
14  
15

16 Corresponding author\*: [ramgeo.in07@gmail.com](mailto:ramgeo.in07@gmail.com); [ramamoorthy@lzu.edu.cn](mailto:ramamoorthy@lzu.edu.cn)  
17

18 **Abstract**

19 Nagaland is part of the northern extension of the Indo-Myanmar range (IMR). This area is  
20 representative of several orogenic upheavals in the Cretaceous-Tertiary that form a relatively  
21 young and mobile land belt. Nagaland is the most recent crustal reaction to the collision of  
22 the Indian and Burmese Plate. Barail formation emerged at the active margin of the Indo-  
23 Burmese plate convergence. The majority of the available tectonic replica proposes that the  
24 malformation and uplift of the Northeastern. We aimed at the highlights of exhumation and  
25 sedimentation, and its other host processes like provenance characteristics of the Barail  
26 sandstones from Nagaland, India. Systematic geological mapping of approximately 50 square  
27 meters has been carried out in the study area. A geological map of the study area was made  
28 on a scale of 1:50,000 in the Indian Topsheet No.58M/4 survey in the Kohima district of  
29 Nagaland. The region was mapped according to need and accessibility by taking the traverses  
30 along the highways, footpaths and across the ranges. In this study, four quarry samples  
31 disseminated in various folds in the Barail Group yielded the ages ranging from  $37.4 \pm 1.5\text{Ma}$   
32 to  $49.9 \pm 2.4\text{Ma}$  and younger than their predecessor sedimentary deposition ages (86.92-  
33 181.81 Ma). The binomial distribution clearly stated that from 46.0 to 32.0Ma, the grain ages  
34 fitted peaks are usually dominated by the young peak. Combined with an interpretation of the

35 origin, the detrital zircon of the young peak age and rocks indicated that most significant  
36 uplifting of the Barail Group occurred during Eocene to the Oligocene, almost timed to  
37 coincide with the colliding of the Indo-Burmese plate more around ~35-50 Ma. Such findings  
38 have been consistent with the current geology of Naga Hills in the province of Nagaland.

39

40 **Keywords:** Detrital Fission Track, Indo-Burmese, Barail sandstones, Exhumation,  
41 Provenance, Northeast India

42

43

#### 44 **Introduction**

45

46 The Indian plate had subducted eastward below the Burma microplate during the India-  
47 Eurasia collision, which is the start point for our understanding of the formation and  
48 evolution of Himalayas-Tibetan Plateau as well as the effects of environment and resources.  
49 Therefore, the onset time of the collision and subduction is one of the hotspots in Geoscience,  
50 however, are still seriously controversial, ranging from the Early Cretaceous to Paleogene  
51 (Evans, 1932; Gupta and Biswas, 2000; Acharyya, 2007, 2010), because the direct and  
52 confidence evidence is rare and poorly yielded. The Indo- Burmese collision have caused the  
53 uplift and exhumation of Nāga Hills, part of the complex mountain barrier on the collision  
54 border (Acharyya, 1986, 2007, 2015; Aitchison, 2019), with the syn-orogenic sedimentation  
55 of Nagaland Hills basin (Brunnschweiler, 1966; Acharyya, 2010; Aitchison et al., 2019) With  
56 the continue colliding of Indian-Burmese plates, This plate margin gives rise to all the  
57 tectonic lithological and relief features typical to the tectonic plate touch zones. For example,  
58 the mountain range chain reveals a variety of concurrent north-south orientation or  
59 subparallel ranges that have intervened by river valleys at present; meanwhile, with the  
60 uplifted of the western Indo-Burmese range, the Nagaland Hills basin was filled with  
61 sediments named Barail group sequences (Evans, 1932; Agrawal and Ghosh, 1986; Gupta  
62 and Biswas, 2000). Subsequently, these molassic sediments were North-East southwest  
63 folded and Elevated in and out of upstanding ridges, giving linearity to the belt with the  
64 defective regional activity and thrusting, representing the compression stress and crustal  
65 shortening The Barail group sequences mostly intercalated with sandstone with shale  
66 formations in the Naga Hills and the provenance analysis, are deeply studied and indicated  
67 that the source rocks (Srivastava, 2013, 2018; Ramamoorthy, 2015, 2016, Odyuo, 2018).  
68 However, their depositional ages are ambiguous, and the regional tectonic settings are poorly

69 known, thus block the further. Interestingly, due to the basin complex tectonic history, lateral  
70 facies variations, scarcity of fossils, and partial reworking of the sedimentary material,  
71 differences still occur in published ages, and thus there is a lack of precise dating.

72

73 Naga Hills part of a complex mountain barricade at the Indo-Burmese boundary. A Northern  
74 extension of the Assam yoma system and it is reaching heights of 3,826 m on the India-  
75 Myanmar border at mount saramati. The Hills obtain heavy rainfall from monsoons and are  
76 naturally clothed with dense forest. Systematic geological mapping of approximately 50  
77 square kilometers has been carried out in the Northeast, Nagaland. In the part of the India  
78 Topsheet No.58M/4 survey in Kohima district of Nagaland. The study area was mapped by  
79 taking traverses along the roads, footpath, and across the ranges according to necessity and  
80 accessibility. A comprehensive analysis of the Barail sediment group in Nagaland using a  
81 combination of origin and ZFT (Zircon fission track) is then presented. ZFT (Zircon fission  
82 track) is a proven method of investigating the lengthy-term background of diverging hillside  
83 belt exhumation (Spiegel., 2000; Bernet., 2001, 2004 a,b) typically used to calculate the  
84 oldest depository age using the youngest or peak age, allowing the reconstruction of the  
85 tectonic evolution of sediment origin (Aoki., 2012, 2014; Beranek & Mortensen, 2011). In  
86 comparison, earlier kinds of research on the ZFT dating of the Naga hill in these regions are  
87 not available. To date, the Naga hills geochronology of sandstones samples India Nagaland  
88 state was not yet explored in detail to define, provenance, and long term exhumation. From  
89 this research paper, we have been using fission-track grain age distribution for detrital zircon  
90 extracted from Naga hill sediments to solve bedrock cooling ages for orogenic origin. Detrital  
91 zircon samples were collected and dated from Barail sandstones in the Naga Hills, Northeast  
92 Nagaland (Figure 1), which document the early deformation of the region. From these  
93 regional perspectives, we suggest a period for the early Cenozoic uplift of the Indo-Burma  
94 collision and growth model, utilizing sedimentary measurements and the findings of the  
95 origin study from the Northeastern Naga Hills. These results can shed more light on the  
96 timing of cooling and exhumation events or periods and enhancing our understanding of the  
97 long-term evolution of Northeast.

98

### 99 **Geological settings**

100

101 Geographically, this study area is a central part of the Indo- Myanmar Range (IMR) and  
102 located in the inner Palaeogene fold belt of Manipur- Nagaland-Upper Assam and Arunachal

103 Pradesh. The most of the stretch of Disang Group with isolated covers with Barail Group  
104 distinguishes the geological setting of the area. Geological provinces are in north-eastern  
105 India mature even after time severance the land of Gondwana. In the collision of Indo-  
106 Burmese plates are during the middle part of the Cretaceous. Gradually, the evolution of  
107 Palaeogene Barail, Surma, Tipam formations are in the regions. Nagaland stratigraphic  
108 formation, altered after Mathur and Evans (1964), the Geology & Mining Directorate (1978),  
109 and Ghose et al.2010), is shown in table .1.

110

111

112 Nagaland rocks are present in the Kohima synclinorium and trending longitudinal belts of  
113 NE-SW. This research study is situated in the western part of the synclinorium. It covers an  
114 extensive area in the intermediate hill ranges of Nagaland. The highest ground of the Patkai  
115 Synclinorium comprises synclines with Barail rocks and the relatively open synclines are  
116 separated by faulted and overthrust Disang shale. Several folds with various types and their  
117 structure describe the area and suggest a variety of malformation events. In addition, faults  
118 are there negotiating from the study area. The study area (94 ° 05'45"N and 25 ° 39'34"E)  
119 which forms the synclinorium of Kohima and includes a group of rocks from Cretaceous to  
120 Eocene Disang (dominantly in clay), followed by the transition sequences from Disang-Barail  
121 (DBTS) (Pandey.N., 1998). It is light grey to grey (Barail sandstone) and has a fine to  
122 medium-grain consistency with occasional shale intercalation.

123

124 The Barail comprises thick sequences of sandstones intercalated with very thin papery shale.  
125 In these rocks, ages from the Upper Eocene to Oligocene, are scattered in patches in  
126 Nagaland (Evans, 1932; Srivastava.S.K, 1998; Gupta and Biswas, 2000). It is exposed in  
127 southern Kohima, the eastern parts of Nagaland, and all along the western margin of the state.  
128 The type area of Barail is limited to the northwest by the Haflong-Disang Thrust trending  
129 roughly NE-SW. It is overlying the Disang. They attain a thickness of about 4000 to 6000 m.  
130 The Barail is divided into three formations in the south and southwest of Nagaland (Evans,  
131 1932) including the Laisong, Jenam, and Renji formations. The Laisong Formation consists  
132 of very hard, grey, thin to thick-bedded sandstones with ferruginous concretions. Occasional  
133 massive sandstones with intercalations of carbonaceous shale are not uncommon. Thin  
134 streaks of coal are also encountered. The thickness of this formation varies from 900 to 2000  
135 m. The Jenam Formation with thicknesses varying from 900 to 2000 m exhibits a gradational  
136 contact with the underlying and overlying formations. The sandstones are dominantly grey to

137 dark grey and thin to thick-bedded with carbonaceous shales. They are commonly  
138 interbedded with silts. The Renji Formation is the youngest member of the Barail Group. This  
139 formation extends into Assam and Manipur. The sandstones are massive, very thick-bedded,  
140 hard and ferruginous, and intercalated with minor shale. They form a thickly forested range  
141 with high peaks such as Japfü (3015 m) in the southwest of Kohima.

142

### 143 **Methods and sampling**

144 Zircon is a common type of rock resistant to weather attacks by physical and chemical. ZFT  
145 is  $\sim 240 \pm 30^\circ\text{C}$  with annealing temperature and the standard orogenic cooling rate is  $15^\circ\text{C}/\text{Myr}$   
146 (Hurford, 1986, Brandon, 1998). Hence Zircon is researching an excellent mineral for its  
147 thermochronology whose rocks are highly essential (Carter, 1999, Bernet, 2005). It has the  
148 superiority to retain knowledge on the current chronology of origin that makes the use of the  
149 ZFT study beneficial for connecting sediment deposits to the uplifting and Orogenic belts  
150 investigation past (Bernet, 2005). In comparison, research data on FT dating and Zircon  
151 length analysis are not yet adequate to enable simulation of the track range (Garver, 1999b).

152

153 Sediment samples have been collected from the Barail Group best exposure along the road.  
154 However, if marked differences in lithological and physical characters were encountered  
155 within a much shorter range, the sampling spacings were also reduced to collect the  
156 representative sample of the rocks. Four systematic sedimentary sandstone samples were  
157 collected from the Northeastern Himalayas in Nagaland. The samples were collected from the  
158 four quarry sections in the Naga Hills (Zubza, Khiruphema, Mezoma, and Jotsoma). Sample  
159 preparation was done by the mineral separation method (Patel RC, Singh P, Lal N (2015)).  
160 The work on zircon mineral separation was carried out at the Department of Geophysics,  
161 Kurukshetra University. We followed international protocols for the use of specific analytical  
162 techniques. We used for separation instruments are disc mill, crusher, and Wiley water table.  
163 We separated a hundred zircon grains from all samples of good quality and equal-sized  
164 (Table 1) by standard, Crushing, Mounting Bromoform, and magnetic separation procedures  
165 of the FTD of Kurukshetra University, India. Zircon grains picked by hand and Grains are  
166 mounted (PFA® Teflon), polished, etched. For etching the Zircon's mineral surface at  $240^\circ\text{C}$   
167 3h, KOH-NaOH chemicals have been used, and the Low Uranium Muscovite has been used  
168 as "external detector" to measure the caused track densities. The FRM-II, thermal column,  
169 Germany conducted sample thermal neutron irradiation. The neutron dosimeter was used for  
170 CN-2 uranium glass. External mediated track detectors (mica) were tested for 5 minutes at 48

171 percent HF at 35 ° C. Spontaneous track densities were examined on internal mineral surfaces  
172 using the Olympus BX-50 with 100 tons of dry lenses and a 1250x total magnification.  
173 Zircon crystals containing prismatic parts parallel to the crystallographic c-axis have been  
174 chosen to measure track densities. By standard zeta method ( $\zeta$ ) Hurford, A.J., Green, P.F.  
175 (1983), and Hurford, A. (1990) Ages with  $\pm 1\sigma$  were determined. The Zeta factor is  
176  $127.61 \pm 4.31$ , which was obtained from the through multiple examinations of the age criteria  
177 for zircon grains. Such as Fish canyon Tuff, Bergell, and Tadree rhyolite.

178

## 179 **Results**

180

181 The present study obtained a limited amount of 50-68 grains from the surface samples and  
182 selected them for the determination of age. Nevertheless, defining the grainage components  
183 ensured definite results. For an example of the  $P(\chi^2) > 5\%$ , age dispersion should be  $\sim 10\%$  the  
184 cooling age, and the pool age will be the same (Snelling, 2005). We find that from the Barail  
185 group age of Eocene-Oligocene (53-33Ma) and ZFT ages were 37 to 49 Ma. In the Barail  
186 sandstones to the east of this depression, the ZFT ages are Cretaceous to Tertiary age (86-58  
187 Ma) and do not appear in the regional pattern. All areas had shown trends of a very similar  
188 age. We had given the results of four quarry samples detailed and summarized in Table 2. It  
189 was shown very clearly from the study that the range and distribution of individual ZFT ages  
190 for each sample appeared within the Radial and Spectrum plots (Figs 2 a, b;  
191 Table 3) and binomial peaks for the measured surface samples shown in (Table 1 and Fig.2c).

192

193 Zubza section was identified as a pooled age is  $37.4 \pm 1.5$  Ma with  $P(\chi^2)$  0.00%. It is derived  
194 from the 50 detrital zircon grains (Table 2; Fig 2c). However, the age dispersion was 0.00%  
195 and individual grains yielded evidence of single-grain ages from  $55.67 \pm 10.7$  Ma to  $29.10 \pm$   
196  $6.1$  Ma (Fig.2a). The histogram shows large spreads over the ages (Figs. 2a-c). The pooled  
197 and central ages are uniform,  $37.4 \pm 1.5$  Ma. ZFT single grain age is derived from a sample of  
198 Jotsoma of Barail Group sediments ranged between  $159.31 \pm 49$  Ma and  $22.24 \pm 5.6$  Ma,  
199 with  $P(\chi^2) = 0.00\%$ . The pooled and central ages are  $44.9 \pm 1.8$  Ma and  $44.5 \pm 1.8$  Ma. Samples  
200 of Khiruphema yielded 46-grain ages, and the age dispersion is 0.00%. Khiruphema pooled  
201 age is  $44.9 \pm 1.8$  Ma as opposed to a central age of  $44.5 \pm 1.8$  Ma, with  $P(\chi^2) = 0.00\%$ . The  
202 Mezoma samples pooled age and central ages are  $51.2 \pm 2.0$  Ma and  $49.9 \pm 2.4$  Ma respectively.  
203 However with the probability density plot shown the well-fitted peaks in Zubza as  $34.5 \pm 0.8$   
204 Ma. The samples of Khiruphema location peaks value as  $46.0 \pm 3.4$  Ma, Mezoma location

205 peak age is  $41.8 \pm 1.6$  Ma, and Jotsoma ages fit peaks shown as  $32.0 \pm 2.6$  Ma. The grain age  
206 range was usually dominated by young peaks, P1, which would have been subject to the  
207 study and ranged from 32.0 to 46.0Ma (Table 3; Fig.2c). There were older peaks present,  
208 32% and 46.5% of the total distribution was present (Fig.2; Table 4).

209

## 210 **Provenance and Long term exhumation**

211

212 Many researchers published about provenance studies in sedimentary rocks over the years  
213 (Schlanke.S (1974), VonEynatten, H (1996, 1999), Schlunegger.F (1998), Garzanti.E, (2008)  
214 Jeffrey M.Amato and Greg H. Mack (2012) Xinchuan Lu (2018). The detrital ZFT can use  
215 the data of provenance analysis (Hurford, A.J (1984, 1991), and Carter. A., (1999), Wei  
216 Wang (2010). Each sample peak age is shown in Table 2, and they are associated with the  
217 times, it can be utilized to distinguish their potential sources of the Barail sediment group in  
218 northeastern Himalayan by comparing to the recent bedrock Fission Track ages (Fig.3). ZFT  
219 grain-age peak can be obtained from source areas where the recent bedrock detrital age of  
220 ZFT is younger or equal to the age of peak and these relationships allow the source area to  
221 contain candidates.

222

223 Generally, the peak ages between 32-46 Ma is importantly from the intensely exhumed  
224 sedimentary rocks of Barail, Nagaland. Detrital grains with freezing ages of around 32 Ma  
225 are insignificantly supplied from Late Eocene to Oligocene. In Figure 3, a contrast of  
226 euhedral, rounded zircons in four quarry parts is shown, which is deposited in the hinterland  
227 basin from 44 to 37 Ma. Because volcanic zircons have a common euhedral grain shape; if  
228 the volcanic input is significant, we expect to find only a strong shape-age relationship with  
229 the 32 Ma cooling age with euhedral grains. There were three hundred euhedral grains of the  
230 cooling age, younger and older euhedral grains, and rounded grains of the same age in each  
231 sample. The strong relationship between solid shape ages, which does not lead all 32Ma  
232 cooling ages to Oligocene Volcanism (Dunkl. I, 2001) have therefore not been confirmed.  
233 The maximum of 30-50 Ma will originate from the Nagaland that was eroded in the late  
234 Eocene-Oligocene from the locations, but it still occurs in parts of the North Eastern  
235 Himalaya.

236

237

238 The evolution of Peak ages in hinterland sediment deposits over time gives us an  
239 understanding of the long-term history of exhumation in Hinterland Naga Hills. Overall, P1  
240 shows the most stable trend since late Eocene (44Ma) and Oligocene (37Ma) in the hinterland  
241 samples. In these result comes about can be point by point in two ways. The primary  
242 alternative is that at a certain time some source regions are expelled and give zircons with  
243 shorter times, but then the rapid exit is shifted to a different area, from which the short-lagged  
244 young zircons are supplied to the basins (Willett, S.D and Brandon, M.T, 2002). This  
245 thermochronology defined the condition as the time-invariant generation of the cooling age  
246 within a given spatial domain. Secondary alternative, zircon sources have been expelled at a  
247 constant rate. Such exhumation rates ought to be set up before reported by the primary event  
248 of detrital zircon with an 8 Myr lag time since none or partially recuperated cover-units must  
249 be removed first to see the young cooling age in the sediment record.

250

251 The crystal clear response is that the sample coverage in the hinterland basin is very  
252 complete, but it is also important that all samples are taken from the Barail group sequences,  
253 which have the benefit of being the best combination and can include all the different Fission  
254 track grain age components revealed at a regional scale in the source area. Samples taken  
255 near the source indicate a more local area, possibly a single surface area, not required by  
256 location in the FT ages of the whole orogenic system (Bernet, 2004a). Source areas can be  
257 located in Nagaland for 46Ma P1 zircon and do not directly affect the exhumation as a result  
258 of normal fault but only erosion. Old peak grains (180 Ma) can only be obtained from  
259 partially restored covered units, such as partially formed zircon P1 in each sample or re-  
260 established.

261

262 The fraction of grains with the Barail sediment cooling age (30 Ma) increases the overtime,  
263 which suggests that the surface area of zircon exposed bedrock with the Barail sediment, may  
264 have increased over time, at least for all the cooling ages, because the exhumation rates are  
265 very stable. With the accessible information, it is not evident how this relates to a possible  
266 alter within the measure of the mountain belt as proposed by researchers. For example,  
267 Schlunegger, F (1999) suggested the elevation mountains at the end of the Eocene to  
268 Oligocene based on the thermochronological details, dynamic modeling, and Cederbom C.E.  
269 (2004) assumed the narrowing of the orogenic system from uplifting and recycling of  
270 hinterland sediments to northeastern of the Himalaya since Eocene to Oligocene.

271

272

273 **Exhumation history of Oligocene to Eocene ages**

274 The cooling period provides a distinct relationship with the long-term exhumation and  
275 deposition of the sediment, whereas the cooling process is closely linked to the uplifting and  
276 exposure of sources' rock (Bernet 2005). Because the time to move erosion and sediments in  
277 comparison (Braun 2006, Brandon 1992) is quite short, the related data can provide the time  
278 delay. The period of delay is characterized as the difference between peak age and the age of  
279 deposition, Garver., (2006), Reiners. P.W (2005, 2007). In the absence of a thermal reset after  
280 burial, the quicker the law lapses the faster and measured the exhumation rate (Bernet, 2005).  
281 Erosion is largely responsible for the exhumation of the upper crustal (6-8 km deep) (Bernet,  
282 2011). Thereafter, all ZFT ages in each sample were taken to represent the Exhumation rate  
283 of the rock source.

284 The interpretation of the time results and the changes in peak age by region can be based on  
285 the binomial fit within the main peaks to establish the historic exhumation status of the Barail  
286 Group. Within the permitted error spectrum, the peak age is about (Table 4) and the time  
287 decreases with the depository age and stays constant for the same strata. We tried to display  
288 peak age averages and measure the time given the effect of small grain counts on each  
289 sample. The Zircons have either placed such a peak;(1) It is extracted from a source rock  
290 which has undergone rapidity; But short-lived, cooling event and then gradually ejected;(2)  
291 recycling from a sediment source, whether the peak age is comparatively old and precedes  
292 oogenesis; or (3) the degradation of dense sections of non- reclaimed volcanic rocks(Bernet,  
293 2011). Moreover in Patkai-Kohima numerous tectonic and sedimentary events occurred in  
294 sync, with plates from India and Burma colliding between about 35 and 50 Ma. The  
295 provenance details and cooling history obtained from sandstone may help to explain the  
296 creation of synchronous exhumation in Patkai-Kohima, where some samples have been dated  
297 so far. 5Ma shows the onset of the rapid evacuation of cooling paths from sandstones. Syntax  
298 regions full cooling histories have been collected for the first time and can be compared to the  
299 cooling and exhumation history of the other areas of the orogeny. This comparison highlights  
300 the similarities and distinctive variations illustrated by the intermediate Patkai-Kohima syntax  
301 between the east boundary of the Indo-Burmese plate and the western compression and  
302 subduction setting. According to our study, the zircon from the northeastern Barail Group  
303 sediments appears to come from Type A, which implies that the Barail Group has undergone

304 a fast increase at 35-50 Ma and then has been exhumed gradually since then. If the  
305 exhumation rate is moderate induces long lead times and poor cooling (Garver. J, 1999b and  
306 Reiners P.W, 2006). The ZFT ( $240 \pm 30$  ° C), broadly dispersed ~40 Ma ZFT period, gradual  
307 exhumation and cooling rate of 4.1°C/myr after a fast, but short, cooling event at ~35-50  
308 Ma, were, by comparison, high closing temperatures. The initial Cenozoic uplift of the  
309 Barail Group took place at ~35-50Ma based on this analysis, based on ZFT results. On the  
310 basis of this ZFT study, a Cenozoic uplift of 35 to 50Ma occurred at the initial Barail group.  
311 In conjunction with the widely recognized Patkai-Kohima tectonic elevation occurrence align  
312 with the early advent of the Indian-Burmese collision by Cenozoic.

### 313 **Conclusions**

314 Detrital zircon FT results of each sample were used for the determination of sediment  
315 provenances and the long term exhumation rates in the Northeastern Nagaland. Sandstones  
316 from the Barail samples of the north-eastern Nagaland regions are conceptually identical,  
317 similar in age distributions, derived from recycled orogenic sources to their detrital zircon  
318 populations. A younger, Oligocene to Eocene, regardless of stratigraphy age, are the  
319 dominant population of the zircon within the sandstones. Four samples of Barail sandstone  
320 show a rather narrow span of central ZFT ages between  $37.4 \pm 1.5$ Ma and  $49.9 \pm 2.4$ Ma. Data  
321 from ZFT and sedimentary areas indicate that the Barail group has only rapid, regional uplift  
322 and cooling age at ~35–50 Ma when detritus material is delivered from northeastern  
323 Nagaland. It is uplifted from the Indian-Burmese collision. Since the Early Cenozoic Cooling  
324 age ~40 Ma, during the Early Cenozoic Cooling age, the Barail formations had a gradual  
325 exhumation and a cooling rate of 4.1°C/Myr. It is worth noting that in the Hinterland basin  
326 the long-term exhumation signals have been deposited over time. The ZFT data provided here  
327 provide no hint that the tectonic or climate structure in Naga Hills has experienced significant  
328 long-term exhumation since the continental crash and seems to be indifferent to 5 Myr. In  
329 Brief, ZFT data shows that the first Cenozoic uplift of the Barail Group occurred in ~35–50  
330 Ma, in conjunction with a widespread tectonic uplift on the Patkai-Kohima synchronous with  
331 the onset of the Indo-Burmese collision during Early Cenozoic period. It concluded that since  
332 the Eocene-Oligocene period the Barail group exhumation pattern is driven by tectonic.

333

334

335

**337 Acknowledgments**

338 The first author RAMAMOORTHY AYYAMPERUMAL gratefully acknowledges the DST  
339 Inspire (Ref.No.dst/inspire/IF140775/Dated.06.12.2014) Government of India, for providing  
340 financial support for this research work. The authors would like thanks to Prof. RC Patel, and  
341 FRM-II Lab Germany for providing Lab facilities and suggestions for research work. We  
342 acknowledge and thanks to careful reviews by Prof.Cristiano Persano, School of earth  
343 sciences, University of Glasgow-UK, and Prof.Xixui Wang, Lanzhou University-China, for  
344 helped us improve the manuscript significantly. The first author is grateful Key Laboratory of  
345 western China's Environmental system, College of earth, and environmental sciences for a  
346 post-doctoral researcher (Award No: 252813, dated 10/04/2020).

**347 References**

- 348 Acharyya, S.K.(2007), Collisional emplacement history of the Naga-Andaman ophiolites and  
349 the position of the eastern Indian suture. *J.Asian Earth Sci.* 29, 229–242.
- 350 Acharyya, S.K.(2010) Tectonic Evolution of Indo-Burma Range with Special Reference to  
351 Naga-Manipur Hills. *Memoir geological society of India No. 75*, pp. 25 - 43
- 352 Acharyya, S.K.(2015), Indo-Burma Range: a belt of accreted microcontinents, ophiolites, and  
353 Mesozoic–Paleogene flyschoid sediments. *Int. J. Earth Sci. (Geol. Rundsch)* 104, K. Lokho et  
354 al. *Journal of Asian Earth Sciences* 101235–1251.
- 355 Acharyya, S.K., Roy, D.K., Mitra, N.D.(1986), Stratigraphy and paleontology of the Naga  
356 Hills Ophiolite Belt. In: *Geology of Nagaland Ophiolite. Geol. Surv. India Mem.* 119, 64–74.
- 357 Aitchison. (2019), Tectonic evolution of the western margin of the Burma microplate-based  
358 on new fossil and radiometric age constraints.*Tectonics*. DOI:10.1029/2018TC005049.
- 359 Aoki, K., Isozaki, Y., Yamamoto, S., Maki, K., Yokoyama, T.,&Hirata, T. (2012), Tectonic  
360 erosion in a Pacific-type orogen: Cretaceous tectonics in Japan. *Geology*, 40, 1087–1090.
- 361 Aoki, K., Isozaki, Y., Kofukuda, D., Sato, T., Yamamoto, A., Maki, K., Hirata, T. (2014),  
362 Provenance diversification within an arc-trench system induced by batholith development:  
363 The Cretaceous Japan case. *Terra Nova*, 26, 139–149.

364 Beranek, L.P., & Mortensen, J.K. (2011), The timing and provenance record of the Late  
365 Permian Klondike orogeny in northwestern Canada and arc-continent collision along with  
366 western North America. *Tectonics*, 30, TC5017. <https://doi.org/10.1029/2010TC002849>.

367

368 Bernet, M., M. Zattin, J.I. Garver, M. Brandon, and J.A. Vance. (2001), Steady-State  
369 Exhumation Of The European Alps, *Geol.*, 29, 35–38

370

371 Bernet, M., and P. Tricart. The Oligocene Orogenic Pulse In The Southern Penninic Arc  
372 (Western Alps): Structural, Sedimentary And Thermochronological Constraints, *Bull. Soc.  
373 Geol. De France*, 182(1), 25–36(2011).

374 Bernet, M., Brandon, M.T., Garver, J.I., and Molitor, B.R. (2004b), Fundamentals of detrital  
375 zircon fission-track analysis for provenance and exhumation studies with examples from the  
376 European Alps, *in* Bernet, M., and Spiegel, C., editors, *Detrital thermochronology –  
377 exhumation and landscape evolution of mountain belts: Geological Society of America  
378 Special Publication*, v. 378, p. 25–36.

379 Bernet, M., Brandon, M.T., Garver, J.I., and Molitor, B.R. (2004a), Downstream changes in  
380 Alpine detrital zircon fission-track ages of the Rhône and Rhine Rivers: *Journal of  
381 Sedimentary Research*, v. 74, p. 82–94.

382

383 Bernet, M., M.T. Brandon, J.I. Garver, and B.R. Molitor. (2004a), Fundamentals Of Detrital  
384 Zircon Fission-Track Analysis For Provenance And Exhumation Studies With Examples  
385 From The European Alps, In *Detrital Thermochronology-Provenance Analysis, Exhumation,  
386 And Landscape Evolution Of Mountain Belts*, Spec. Publ., Vol. 378, Edited By M. Bernet  
387 And C. Spiegel, Pp. 25–36, *Geol. Soc. Am.*, New York

388 Bernet, M., Zattin, M., Garver, J.I., Brandon, M.T., and Vance, J.A. (2001), Steady-state  
389 exhumation of the European Alps: *Geology*, v. 29, p. 35–38.

390

391 Bernet, M.J., I. Garver. (2005), Fission-Track Analysis of Detrital Zircon, *Rev. Mineral.  
392 Geochem.*, 8(58), 205–238.

393

394 Blanckenburg, F.Von & Davies, J.H. (1995), Slab Break; A Model For Syncollisional  
395 Magmatism And Tectonics In The Alps. *Tectonics*, 14, 120-131.  
396

397 Brandon, M., and J.A.Vance. (1992), New Statistical Methods For Analysis Of Fission Track  
398 Grain-Age Distributions With Applications To Detrital Zircon Ages From The Olympic  
399 Subduction Complex, Western Washington State, *Geol. Soc. Am. Bull.*, 292, 565–636.  
400

401 Brandon.M., Garver, J. (1998), Late Cenozoic Exhumation Of The Cascadia Accretionary  
402 Wedge In The Olympic Mountains, Northwest Washington State. *Geological Society of  
403 America Bulletin*, 110, 985-1009.  
404

405 Braun, J., Der Beek, Van, P., Batt, G. E. (2006), *Quantitative Thermochronology*. Cambridge  
406 University Press. Reiners, P. W., and M. T. Brandon (2006) Using Thermochronology To  
407 Understand Orogenic Erosion, *Annual Review Of Earth And Planetary Sciences*, 34, 419–  
408 466  
409

410 Carter, A. And Moss, S.J. (1999), Combined Detrital-Zircon Fission-Track And U-Pb Dating:  
411 A New Approach To Understanding Hinterland Evolution. *Geology*, 27, 235-238

412 Cawood, P. A., Hawkesworth, C. J., & Dhuime, B. (2012), Detrital zircon record, and  
413 tectonic setting. *Geology*, 40, 875–878.  
414

415 Cederbom, C.E., Sinclair, H.D., Schlunegger, F. And Rahn, M.K. (2004), Climate-Induced  
416 Rebound And Exhumation Of The European Alps. *Geology*, 32, 709-712

417 Chen, M., Sun, M., Cai, K., Buslov, M. M., Zhao, G., Jian, Y., Voytishkek, E. E. (2016), The  
418 early Paleozoic tectonic evolution of the Russian Altai: Implications from geochemical and  
419 detrital zircon U–Pb and Hf isotopic studies of meta-sedimentary complexes in the Charysh–  
420 Terekta–Ulagan–Sayan suture zone. *Gondwana Research*, 34, 1–15.  
421

422 Dunkl, I., Di Giulio, A. & Kuhlemann, J.(2001), Combination Of Single-Grain Fission-Track  
423 Chronology And Morphological Analysis Of Detrital Zircon Crystals In Provenance Studies -  
424 Sources Of The Macigno Formation (Apennines, Italy). *J. Sediment. Res.*, 71, 516-525.

425 Ehlers, T., Chaudhri, A., Kumar, S., Fuller, C. W., Willett, S. D., Ketcham, R. A., Brandon,  
426 M. T., Belton, D. X., Kohn, B. P., Gleadow, A. J. W., Dunai, T. J., Fu, F. Q. (2005),  
427 Computational Tools For Low-Temperature Thermochronometer Interpretation. *Reviews In*  
428 *Mineralogy & Geochemistry*, 58, 589-622.

429 Falkowski, S., Enkelmann, E., & Ehlers, T. A. (2014), Constraining the area of rapid and  
430 deep-seated exhumation at the St. Elias syntaxis, Southeast Alaska, with detrital zircon  
431 fission-track analysis. *Tectonics*, 33, 597–616.

432 Fujisaki, W., Isozaki, Y., Maki, K., Sakata, S., Hirata, T., & Maruyama, S. (2014), Age  
433 spectra of detrital zircon of the Jurassic clastic rocks of the Mino-Tanba AC belt in SW  
434 Japan: Constraints to the provenance of the mid-Mesozoic trench in East Asia. *Journal of*  
435 *Asian Earth Sciences*, 88, 62–73.

436

437 Garver, J., M. T. Brandon, M. K. Roden-Tice, And P. J. J. Kamp. (1999b) Exhumation  
438 History Of Orogenic Highlands Determined By Detrital Fission Track Thermochronology, In  
439 *Exhumation Processes: Normal Faulting, Ductile Flow, And Erosion*, Spec. Publ., Vol. 154,  
440 Edited By U. Ring Et Al., Pp. 283–304, Geol. Soc., London.

441

442 Garver, J.I., Brandon, M.T., Roden-Tice, M.K. & Kamp, P.J.J. (1999), Exhumation History  
443 Of Orogenic Highlands Determined By Detrital Fission Track Thermochronology. In:  
444 *Exhumation Processes: Normal Faulting, Ductile Flow, and Erosion* (Ed. Byu. Ring, Et Al.)  
445 *Geol. Soc. (London) Spec. Publ.*, 154, 283-304.

446

447 Garzanti, E. & Malusa', M.G. (2008), The Oligocene Alps: Domal Unroofing And Drainage  
448 Development During Early Orogenic Growth. *Earth Planet. Sci. Lett.*, 286, 487-500.

449

450 Granger, D.E., Kirchner, J.W. & Finkel, R. (1996), Spatially Averaged Long-Term Erosion  
451 Rates Measured From In Situ Produced Cosmogenic Nuclides In Alluvial Sediment. *J.*  
452 *Geol.*,104, 249-257.

453

454 Grasemann, B., And Mancktelow, N.S. (1993), Two–Dimensional Thermal Modelling Of  
455 Normal Faulting: The Simplon Fault Zone, Central Alps, Switzerland. *Tectonophysics*, 225,  
456 155-165.

457 Gupta, A.B., Biswas, A.K. (2000), Geology of Assam. Geol. Soc. Ind. Bangalore, pp. 1–169.

458 Hofmann, H., Grey, K., Hickman, A., Thorpe, R. (1999), Origin of 3.45 Ga coniform  
459 stromatolites in the Warrawoona Group, Western Australia. Geol. Soc. Am. Bull. 111,1256–  
460 1262.

461 Hampton, B. A., Ridgway, K. D., & Gehrels, G. E. (2010), A detrital record of Mesozoic  
462 island arc accretion and exhumation in the North American Cordillera: U-Pb geochronology  
463 of the Kahiltna basin, southern Alaska. *Tectonics*, 29, TC4015. <https://doi.org/10.1029/2009TC00>  
464 25-44.

465 Han, Y., Zhao, G., Sun, M., Eizenhöfer, P. R., Hou, W., Zhang, X., Zhang, G. (2015),  
466 Paleozoic accretionary orogenesis in the Paleo-Asian Ocean: Insights from detrital zircons  
467 from Silurian to Carboniferous strata at the northwestern margin of the Tarim Craton.  
468 *Tectonics*, 34, 334–351.

469

470 Hinderer, M. (1999), Late Quaternary And Modern Denudation Of The Alps And  
471 Implications For Climate Controlled Erosional Processes. *Tübinger Geowissenschaft. Arb.*,  
472 Ser. A, 52, 70.

473

474 Hinderer, M. (2001), Late Quaternary Denudation Of The Alps, Valley And Lake Fillings  
475 And Modern River Loads. *Geodin. Act.*, 14, 231-263.

476 Hu, L., Cawood, P. A., Du, Y., Yang, J., & Jiao (2015), Late Paleozoic to Early Mesozoic  
477 provenance record of Paleo-Pacific subduction beneath South China. *Tectonics*, 34, 986–  
478 1008.

479

480 Hurford Ja, A.J., Fitch, F.J., and Clarke.A. (1984), Resolution Of The Age Structure Of The  
481 Detrital Zircon Populations Of Two Lower Cretaceous Sandstones From The Weald Of  
482 England By Fission Track Dating. *Geol. Mag.*, 121, 269-277

483

484 Hurford, A. (1986), Cooling And Uplift Patterns In The Lepontine Alps, South Central  
485 Switzerland And An Age Of Vertical Movement On The Insubric Fault Line, *Contrib.*  
486 *Mineral. Petrol.*, 92, 413–427.

487

488 Hurford, A.J. And Carter, A. (1991), The Role Of Fission Track Dating In Discrimination Of  
489 Provenance. In: Developments in Sedimentary Provenance Studies (Ed. By A.C. Morton, S.P.  
490 Todd& P.D.W. Haughton), Geol. Soc. Spec. Publ., 57, 67-78

491 Hurford, A.J., Green, P.F (1983), Zeta Age Calibration of Fission-Track Dating. *Isotope*  
492 *Geoscience*, 1,285-317.

493

494 Hurford, A. (1990), Standardization Of Fission Track Dating Calibration: Recommendation  
495 By The Fission Track Working Group Of The I.U.G.S.Subcommission On Geochronology.  
496 *Chemical Geology*, 80, 171-178.

497

498 Hurford.A (1986), Cooling And Uplift Patterns In The Lepontine Alps, South Central  
499 Switzerland And An Age Of Vertical Movement On The Insubric Fault Line, *Contrib.*  
500 *Mineral. Petrol.*, 92, 413–427.

501 Jeffrey M. Amato and Greg H. Mack. (2012), Detrital zircon geochronology from the  
502 Cambrian-Ordovician Bliss Sandstone, New Mexico: Evidence for contrasting Grenville-age  
503 and Cambrian sources on opposite sides of the Transcontinental Arch, *GSA Bulletin*;  
504 November/December; v. 124; no. 11/12; p. 1826–1840; DOI:10.1130/B30657.1.

505 Jiao, R., Seward, D., Little, T. A., & Kohn, B. P. (2014), Thermal history and exhumation of  
506 basement rocks from Mesozoic to Cenozoic subduction cycles, central North Island, New  
507 Zealand. *Tectonics*, 33, 1920–1935.

508

509 Kuhlemann, J., Frisch, W., Dunkl, I. & Szekely, B. (2001), Quantifying Tectonic Versus  
510 Erosive Denudation by the Sediment: The Miocene Core Complex Of The Alps.  
511 *Tectonophysics*,330, 1-23.

512

513 Kuhlemann, J., Frisch, W., Szekely, B., Dunkl, I.& Kazmer, M. (2002), Post-Collisional  
514 Sediment Budget History Of The Alps: Tectonic Versus Climatic Control. *Int. J. Earth Sci.*,  
515 91,818-837.

516

517 Lindsay, J.F., Holiday D.W. And Hulbert, A.G. (1991), Sequence stratigraphy and the  
518 evolution of the Ganges-Brahmaputra delta complex; Amer. Assoc. Petrol. Geol. Bull., v.75,  
519 pp.1233-1254.  
520  
521

522 Mhabemo Odyuo. (2018), Petrography and geochemistry of middle Implications on the  
523 depositional environment, provenance, paleoweathering, and bhuban formation Nagaland,  
524 India: tectonic settings. International research journal of earth sciences. Vol. 6(1), 1-11,  
525

526 Pandey, N., And Srivastava, S.K. (1998), A Preliminary Report On Disang-Barail Transition,  
527 North West Of Kohima, Nagaland, (Abs.). Workshop On Geodynamics And Natural  
528 Resources Of North East India, Dibrugarh, Pp.24  
529

530 Patel RC, Singh P, Lal Nb. (2015), Thrusting And Back-Thrusting As Posted Placement  
531 Kinematics Of The Almora Klippe: Insights From Low-Temperature Thermochronology.  
532 Tectonophysics 653:41–51.  
533

534 Ramamoorthy.A. (2015), Petrography and Provenance of surface barail sandstones, Kohima,  
535 Nagaland, Int.Jour.LTEMASVol.4.Issue10..Pp.35-41.  
536

537 Ramamoorthy.A. (2016), Petrography And Heavy Mineral Analysis Of Barail Sandstones,  
538 Zubza Village, Kohima District, Nagaland India, Int Jour.Geo.Ear.Sci.Vol.2.No.3.Pp-43-53.  
539

540 Reiners, P. W., And M. T.Brandon. (2006) Using Thermochronology To Understand  
541 Orogenic Erosion, Ann. Rev. Earth Planet. Sci., 34, 419–66.  
542

543 Ruiz, G., D.Seward, and W.Winkler. (2004), Detrital Thermochronology—A New  
544 Perspective On Hinterland Tectonics, An Example From The Andean Amazon Basin,  
545 Ecuador, Basin Res., 16, 413–430.  
546

547 Schlanke, S. (1974), Geologie Der Subalpinen Molasse Zwischen Biberbrugg Sz, Huetten Zh  
548 Und Aegerisee Zg, Schweiz. Eclog. Geol. Helvet., 67, 243-331.  
549

550 Schlunegger, F. And Willett, S.D. (1999), Spatial and Temporal Variations In Exhumation Of  
551 The Central Swiss Alps And Implications For Exhumation Mechanisms. In: Exhumation  
552 Processes: Normal Faulting, Ductile Flow, and Erosion (Ed. By U. Ring, Et Al.) Geol. Soc.  
553 (London) Spec. Publ., 154, 157-179.

554

555 Schlunegger, F., Slingerland, R. And Matter, A. (1998), Crustal Thickening And Crustal  
556 Extension As Controls On The Evolution Of The Drainage Network Of The Central Swiss  
557 Alps Between 30 Ma And The Present; Constraints From The Stratigraphy Of The North  
558 Alpine Foreland Basin And The Structural Evolution Of The Alps. Basin Res., 10, 197-212.

559

560 S.K.Srivastava. (2013), Petrography and Major Element Geochemistry of Oligocene Barail  
561 Sediments in and around Jotsoma, Kohima, Nagaland Gond.Geol. Mag., V. 28(2), December  
562 2013. pp.159-164.

563

564 S.K.Srivastava. (2018), Petrography and major element Geochemistry of Paleogene  
565 sandstones, KohimaTown, Nagaland.Journal of Applied Geochemistry, Vol.20, No.1.pp41-  
566 49.

567 Stüwe, K., White, L., Brown, R. (1994) The Influence of Eroding Topography On Steady-  
568 State Isotherms. Application to Fission Track Analysis, Earth Planetary Science Letters, 124,  
569 63-74.

570 Sueoka, S., Kohn, B. P., Tagami, T., Tsutsumi, H., Hasebe, N., Tamura, A., & Arai, S.  
571 (2012), Denudation history of the Kiso Range, central Japan, and its tectonic implications:  
572 Constraints from low-temperature thermochronology. Island Arc, 21, 32–52.

573 Tsutsumi, Y., Miyashita, A., Horie, K., & Shiraishi, K. (2012). Existence of multiple units  
574 with different accretionary and metamorphic ages in the Sanbagawa Belt, Sakuma–Tenryu  
575 area, central Japan. Island Arc, 21, 317–326.

576 Von Eynatten, H., Gaupp, R. And Wijbrans, J.R. (1996),  $^{40}\text{Ar}/^{39}\text{Ar}$  Aser-Probe Dating Of  
577 Detrital White Micas from Cretaceous Sedimentary Rocks of The Eastern Alps; Evidence For  
578 Variscan High-Pressure Metamorphism And Implications For Alpine Orogeny. Geology, 24,  
579 691-694.

580

581 Von Eynatten, H., Schlunegger, F. And Gaupp, R. (1999), Exhumation Of The Central Alps:  
582 Evidence From  $^{40}\text{Ar}/^{39}\text{Ar}$  Laserprobe Dating Of Detrital White Micas From The Swiss  
583 Molasse Basin. *Terra Nova*, 11, 284-289.

584 Wei Wang. (2010), Detrital Zircon Ages and Hf-Nd Isotopic Composition of Neoproterozoic  
585 Sedimentary Rocks in the Yangtze Block: Constraints on the Deposition Age and  
586 Provenance, *The Journal of Geology* Vol. 118, No. 1, pp. 79-94

587 Willett, S.D. And Brandon, M.T. (2002), On Steady- States In Mountain Belts. *Geology*, 30,  
588 175-178

589 Xinchuan Lu. (2018), U-Pb Detrital Zircon Geochronology of Late Triassic to Early Jurassic  
590 Sandstones in the Northwestern Junggar Basin and its Implications. Lu et al., *J Geol Geophys*  
591 7:1DOI: 10.4172/2381-8719.1000320.

592

593

594

595

596

597

598

Figure 1,2,3.

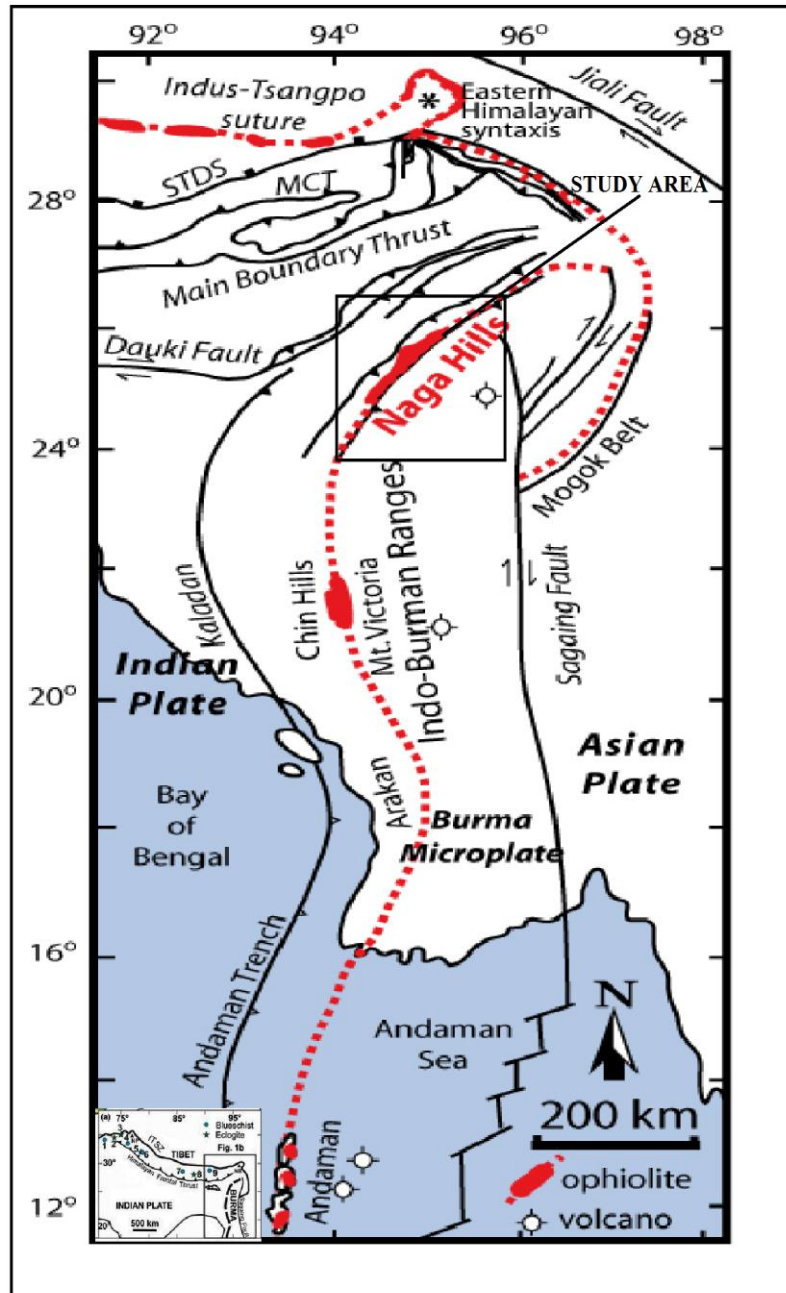
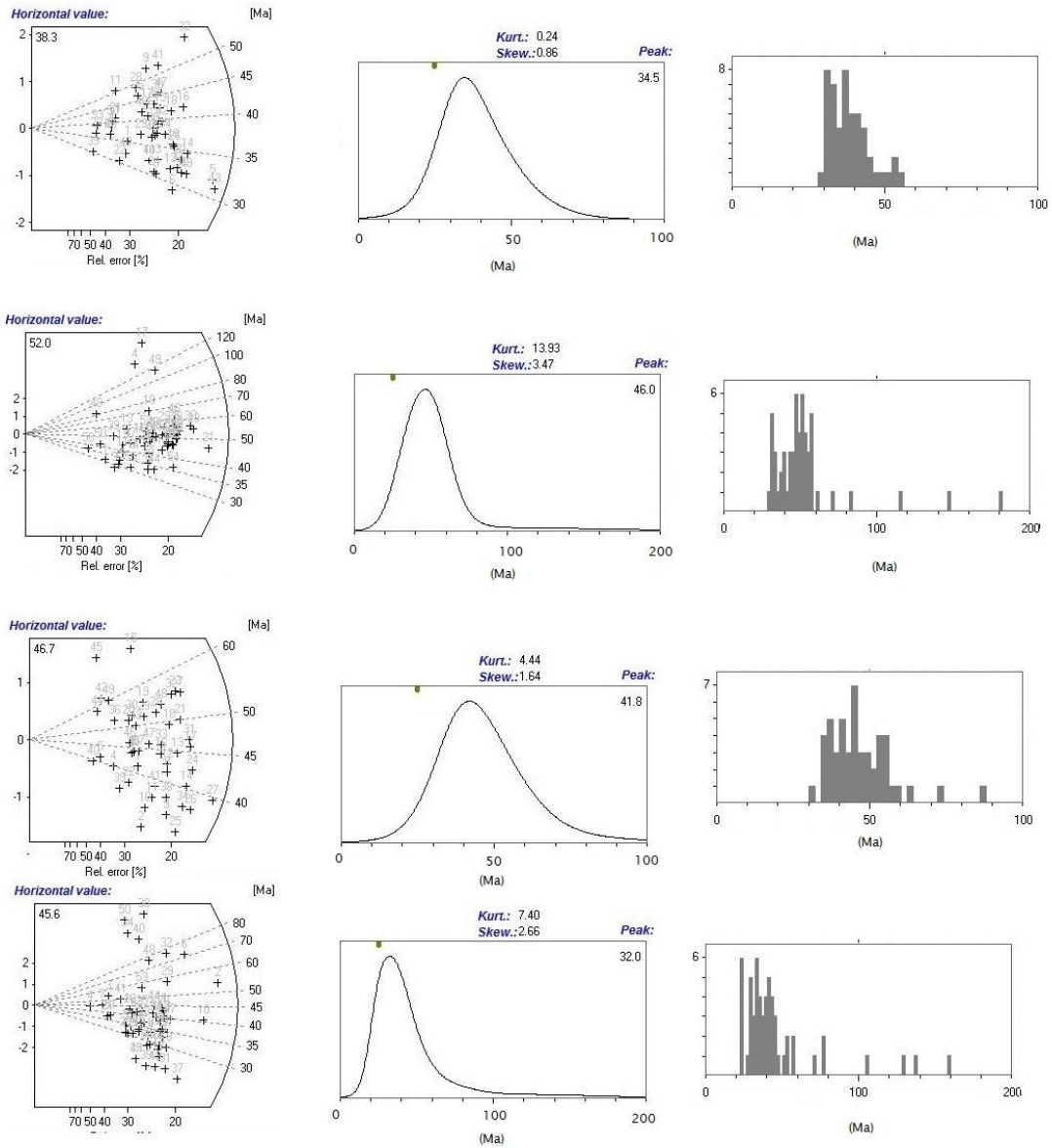


**Fig.1.** Simplified tectonic map of Nagaland and its surrounding areas (Modified by Nilan Chatterjee, 2014)



**Figs. 2 a,b,c.** Detrital zircon fission-track radial plots and single-grain age and decomposed age distributions for the northeastern Barail formation; the black crosses represent single-grain ages, gray dashed lines are the curves of observed grain age distributions, and bold lines are the curves of binomial best fit peaks; peak fitting follows Galbraith and Green (1990) and Brandon (1996) using BINOMFIT (Brandon, 1992).

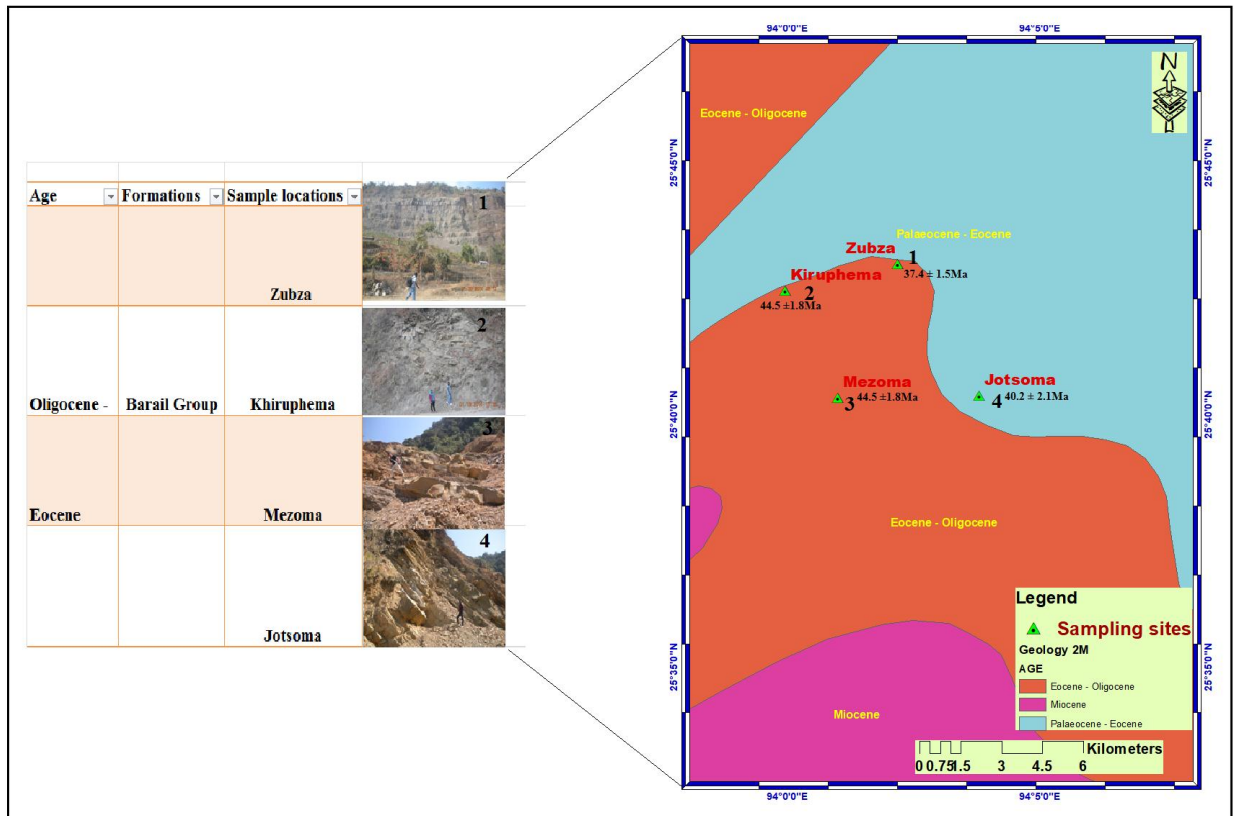


**Fig. 3.** Geological Map of the Nagaland showing evidence of rejuvenation or initiation of tectonic activity at ~35–50 Ma.

**Table 1.** Generalized stratigraphic succession of Nagaland, Eastern Himalaya (after Mathur and Evans, 1964; Agrawal and Ghosh, 1986; GSI, 1978; Gupta and Biswas, 2000, 2010)

Age	Group/Sub-Group	Formation and Thickness in metre	Lithology
Pleistocene to Holocene	Alluvium	Alluvium	Gravels, silts, and clays
Pleistocene	Dihing	Dihing (300-1600m)	Pebbles, Cobbles, and boulders of sandstone in a ferruginous coarse sandy matrix.
Pliocene to Pleistocene	Dupitila	Namsang (800m)	Sandstone, coarse occasionally pebbly gritty with mottled clay bands.
Miocene to Pliocene	Tipam	Girujan clay	Mottled clays, shales of varied colours with medium to fine-grained sandstone.
		1200 –2300 Tipam s.st	Massive sandstone, medium to coarse-grained with current bedded structures
Miocene	Surma	Bokabil (400m)	Alternations of shales with siltstone and sandstone.
		Upper Bhubhan (400m)	Alternations of sandstone and shale. Silty shale with sand lenticels, sandstone medium-grained soft with current ripples.
		Middle Bhubhan (450m)	
Late Eocene to Oligocene	Barail	Renji (900m)	Sandstone medium to thick-bedded, fine-grained, well sorted. Occasional carbonaceous shales.
		Jenam (850m)	Shales with subordinate sandstone; Sandstones occur as lenticular bodies and as thin bands.
		Laisong (1750m)	Sandstone with minor silty shale. Sandstone thin to thick-bedded.
		Upper (1800-3000m)	Dark grey, splintery shale with non-calcareous siltstone and silty sandstone.
Cretaceous to Eocene	Disang	Lower	metamorphosed sediments of slates, phyllites with lenticular limestone beds. Ophiolites



**Table. 2.** Detrital Zircon Fission Track Dating Results for the Barail Group

Sample name	Location	Elevation	Nc	$\rho_s$ (105/cm)	$\rho_i$ (105/cm)	$\rho_d$ (105/cm)	P( $\chi^2$ ) (%)	Central age
				(Ns)	(Ni)	(Nd)		(Ma) ( $\pm 1\sigma$ )
Zubza	25°44.235'	907	50	3.79E+06	2.42E+06	3.84E+05	0	37.4 $\pm$ 1.5
Khiruphema	25°43.855'	994	46	6.20E+06	3.33E+06	3.84E+05	0	44.5 $\pm$ 1.8
Mezoma	25°40.520'	1443	56	7.27E+06	3.52E+06	3.84E+05	0	44.9 $\pm$ 2.4
Jotsoma	25°39.548'	1716	68	5.56E+06	3.22E+06	3.84E+05	0	40.2 $\pm$ 2.1

Nc = number of zircon crystals analyzed. P( $\chi^2$ ) = the probability of  $\chi^2$  for  $\nu$  degrees of freedom (where  $\nu=Nc-1$ ) [Galbraith, 1984]. The age calibration standard used was Fish Canyon Tuff zircon (28Ma); the CN glasses prepared by J. Schreurs at Corning Inc., Corning (New York) was used as a dosimeter to measure the neutron fluencies during irradiation. All analyses were performed by Wanming Yuan, who employed a personal weighted mean zeta while using the above methods and standards.



**Table. 3.** Decomposed Results of Detrital Zircon Fission Track Grains and Peak ages

	Strata range (Ma)	N	Young Peak age	Old Peak age	Age range (Ma)	Mean age, Width, and Size of best peaks
<b>Sample Locations</b>						<b>Peak (ma)</b>
Zubza						34.5±0.8
	33-56	50	34.5	-	29.10-55.67	W=0.92
						Nf=46.5%
Khiruphema						46.0±3.4
	33-56	46	46	86.92	31.68-86.92	W=0.62
						Nf=32%
Mezoma						41.8±1.6
	33-56	56	41.8	181.81	28.52-181.81	W=0.87
						Nf=35%
Jotsoma						32.0±2.6
	33-56	68	32	159.31	26.25-159.31	W=0.4
						Nf=42%

**N-the total number of grains counted; binomial peak fit age has given are a  $\pm 2\sigma$  error.**

**The percentage of grains in a specific peak is also given.**

